AIP | Applied Physics Letters

Evidence of percolation related power law behavior in the thermal conductivity of nanotube/polymer composites

B.-W. Kim, S.-H. Park, R. S. Kapadia, and P. R. Bandaru

Citation: Applied Physics Letters **102**, 243105 (2013); doi: 10.1063/1.4811497
View online: http://dx.doi.org/10.1063/1.4811497
View Table of Contents: http://scitation.aip.org/content/aip/journal/apl/102/24?ver=pdfcov
Published by the AIP Publishing

Evidence of percolation related power law behavior in the thermal conductivity of nanotube/polymer composites

B.-W. Kim, S.-H. Park, R. S. Kapadia, and P. R. Bandaru
Program in Materials Science, Department of Mechanical and Aerospace Engineering, University of California, San Diego, La Jolla, California 92093, USA

(Received 8 April 2013; accepted 4 June 2013; published online 18 June 2013)

A power law relation for the thermal conductivity, indicative of percolation, is reported through measurements on carbon nanotube/polymer composites. Our results contradict earlier assertions and indicate that synthesis methodologies may be adapted to facilitate such behavior. Consistent modeling of the experimentally determined electrical and thermal conductivity anisotropy, in addition to the incorporation of interfacial resistance, was used to understand the underlying mechanisms and variations. © *2013 AIP Publishing LLC*. [http://dx.doi.org/10.1063/1.4811497]

The large length to diameter aspect ratio of one dimensional nanostructures such as carbon nanotubes (CNTs) or nanowires is expected to enhance both the electrical conductivity (σ) and thermal conductivity (κ) of insulating matrices, e.g., polymers, at relatively low nanostructure filler fractions. Integral to such possible enhancement are (i) the postulated high conductivity of the nanostructures along the length of the wires, due to the reduced scattering space/probability,[1,2] and (ii) the aspect that the fillers span/percolate the matrix. Moreover, it would be expected that the anisotropy in the σ and the κ of the fillers would be transferred to the composite and the study of concomitant effects, together with issues related to thermal percolation, is discussed in this letter. Such investigations would have wide implications to a wide variety of envisaged applications of nanostructure/polymer composites incorporating structural reinforcement,[3] electromagnetic interference (EMI) shielding,[4,5] electrochemical capacitors,[6] etc.

In this study, multi-walled CNTs (of average length 1.6 μm and diameter of 45 nm, with standard deviations of 0.5 μm and 14 nm, respectively, yielding an average length/diameter aspect ratio—*A.R.*, of ~35) in a range of volume fractions (ϕ), i.e., 1–10 vol. % (higher fractions rendered the composites brittle) were dispersed uniformly in a reactive ethylene terpolymer (RET) matrix through a careful blend of solution processing and mixing techniques—as outlined in Figure 1. The uniformity of the dispersion was gauged through (a) considering the nanostructure dispersion, through scanning electron microscopy (SEM) micrographs at various length scales (1 μm−100 μm), as well as through (b) our development and use of a image processing algorithm for comparing the given distribution to a preferred (e.g., uniform) distribution.[7] The underlying rationale for the choice of the RET was that ester bond linkages between the carboxyl groups on acid functionalized CNTs and the epoxide groups on the polymer would enable robust bonding, and was verified through Fourier transform infrared (FTIR) spectroscopy.[8] Consequently, both functionalized CNTs and RET were solubilized in toluene solvent and blended through ultrasonication. The blend was cast into a glass Petri dish, where the excess solvent was removed by heat treatment in a furnace—further details of the composite synthesis technique have been previously published.[9] The obtained composite was removed from the dish and then stacked and subject to a hot press treatment to obtain CNT/RET films/plates of the desired thickness. We report electrical and thermal measurements on representative composite plates of 2 mm thickness.

Four probe measurements were used for the σ ($=x/RA$, evaluated from the measured electrical resistance R, with x as the contact spacing and A as the cross-sectional area) of the composites with $R < 1\,\text{G}\Omega$, while for higher resistance composites two-point measurements (using the Agilent B1500A semiconductor device analyzer, with triaxial probes) were employed. The composites were subject to mild oxygen plasma treatment to remove surface contamination and subsequently, 5–10 nm of Ti followed by 100 nm of Au were sputtered on for electrical contacts. For measurements of the *in-plane* conductivity ($\sigma_{\|}$), the contacts were on the *either side* of the composite, while measurements of the *cross-plane* (/through thickness) conductivity ($\sigma_{\perp}$) used contacts deposited on the *top* and *bottom* of the composite—see Figure 1(d). Self-heating was negligible due to the low applied power.

The measured $\sigma_{\|}$ and $\sigma_{\perp}$ as a function of the CNT concentration is plotted in Figure 2. The variation of both $\sigma_{\|}$ and $\sigma_{\perp}$ could be fitted to power law relations of the form[10]

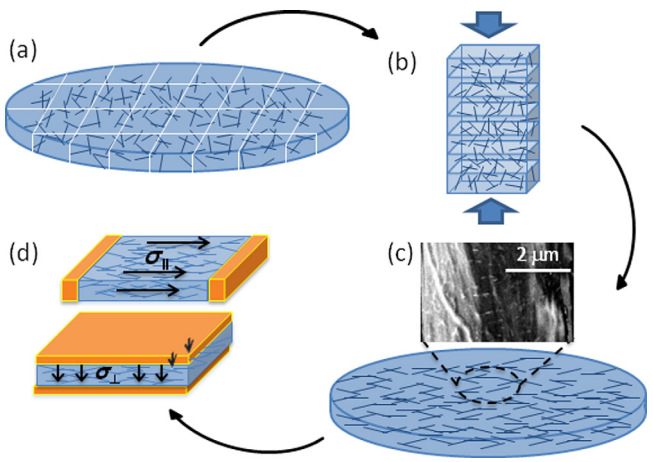

FIG. 1. (a) Blended CNT/polymer composite material was diced and (b) subject to repeated compressive stress. (c) The compressed sheet comprises CNTs preferentially aligned in the plane of the sheet. (d) *In-plane* (top) *and cross-plane* (bottom) electrical and thermal conductivity measurements were carried out to ascertain anisotropy and percolation.

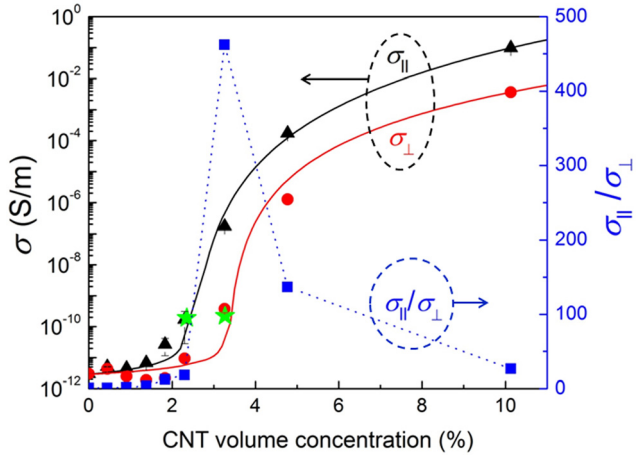

FIG. 2. The variation of the measured electrical conductivity with added CNT filler concentration depicted for the *in plane* ($\sigma_{\parallel}$) and *cross plane* ($\sigma_{\perp}$) configurations. The anisotropy ratio, i.e., $\sigma_{\parallel}/\sigma_{\perp}$ is indicated on the right hand axis. The * indicates the results of the Straley model relating the product of the *electrical* resistances of the matrix and the filler to the percolation threshold.

$$\sigma_{DC} \sim \begin{cases} (\phi_c - \phi)^{-s}, & \phi < \phi_c \\ (\phi - \phi_c)^{t}, & \phi > \phi_c, \end{cases} \tag{1}$$

where ϕ_c is the threshold volume fraction for electrical percolation, while s and t are critical exponents. We also estimated, the threshold from excluded volume percolation theory,[11,12] for CNTs with an aspect ratio ($A.R.$) of ~35, using

$$\phi_c(A.R.) = \frac{C}{\frac{4\pi}{3} + 2\pi(A.R.) + \frac{\pi}{2}(A.R.)^2}\left[\frac{\pi}{6} + \frac{\pi}{4}(A.R.)\right]. \tag{2}$$

C is a constant in the range of 1.4 (for thin rods) to 2.8 (for spherical objects).[13] Using $C \sim 1.4$, for the nanotubes, a ϕ_c of ~2.2 vol. % was estimated. While the fitted ϕ_c was ~2.3 vol. % for the $\sigma_{\parallel}$ change, a value of ~3.3 vol. % was noted for the $\sigma_{\perp}$ variation. Moreover, there was a more gradual ($t \sim 4.2$ for $\sigma_{\perp}$ compared with a t value ~5.7 for the $\sigma_{\parallel}$ variation[14]) and smaller net increase. The differing values of ϕ_c for the $\sigma_{\perp}$ and $\sigma_{\parallel}$ indicate anisotropy and the $\sigma_{\parallel}/\sigma_{\perp}$ ratio has been indicated in Figure 2, e.g., the larger value for $\sigma_{\perp}$ could be tentatively understood from the greater deviation from isotropic arrangement[15,16] of the nanotubes.

Concomitantly, the *cross plane* ($\kappa_{\perp}$) and *in-plane* ($\kappa_{\parallel}$) thermal conductivity values were estimated through a steady state method and the 3ω methodology,[17] respectively. For $\kappa_{\perp}$ the experimental apparatus was modeled and constructed in accordance with ASTM (American Society for Testing and Materials) standards E1225 and D 5470. The accuracy of measurement was estimated to be ~3% through comparison with standards. For the $\kappa_{\parallel}$ measurements, employing the 3ω technique, Ti/Au metal lines (70 μm wide and 10 mm long) which serve as both heater and thermometer were deposited on the composites, with the length scales chosen so as to approximate a narrow line heat source[18,19] (with a ratio of the sample thickness to the metal line width of ~30). Using a lock-in amplifier (Stanford Research Systems: SR 830) and a Wheatstone bridge setup, alternating current, $I(\omega)$, of angular frequency ω (with frequencies (f) in the range of 0.1 Hz-1000 Hz), passed through the metal lines induces resistance oscillations at 2ω: $R(2\omega)$, due to Joule heating ($\sim I^2R$), from which the thermal conductivity can be deduced from the third harmonic voltage, $V(3\omega)$ ($=I(\omega)R(2\omega)$). The temperature change (ΔT) was deduced using the relation:[17] $\Delta T = \frac{2V(3\omega)}{\alpha V(\omega)}$, where α is the measured temperature coefficient of resistance of the metal line. Assuming an adiabatic boundary condition at the bottom of the composite (which is valid for a thermal penetration depth smaller than 2 mm (Ref. 19)), the estimated ΔT could be then related to the thermal conductivity product, $\kappa_{\parallel} \cdot \kappa_{\perp}$, obtained through

$$\Delta T \cong \frac{P}{2\pi\sqrt{\kappa_{\parallel} \cdot \kappa_{\perp}}}[-\ln(\omega) + G]. \tag{3}$$

In Eq. (3), P is the electrical power per unit length of the heater and G is a constant. Combining the steady-state and the 3ω measurements, the individual values of $\kappa_{\parallel}$ and $\kappa_{\perp}$ were computed. Generally, the CNTs are covered by the polymer and the surface of the composites is not electrically conducting. We ensure that the sample and the metal lines are electrically isolated/mutually insulated at all CNT concentrations through monitoring the electrical capacitance (for possible shorting) as well as through the variation of the temperature change/oscillation (ΔT) with frequency (f). While insulated samples exhibit a well-predicted variation, non-insulated samples (e.g., a bare Si substrate) exhibit irregular behavior.

The measured $\kappa_{\perp}$ and the estimated $\kappa_{\parallel}$ are then plotted as a function of the CNT concentration in Figure 3 along with the $\kappa_{\parallel}/\kappa_{\perp}$ anisotropy ratio. While a fairly linear change was noted for $\kappa_{\perp}$, a percolation like behavior, similar to the variation in σ, was observed in $\kappa_{\parallel}$. We then attempted to fit the $\kappa_{\parallel}$ variation using expressions of the form

$$\kappa_{\parallel} \sim \begin{cases} (\phi_{c,k} - \phi)^{-p}, \phi < \phi_{c,k} \\ (\phi - \phi_{c,k})^{q}, \ \phi > \phi_{c,k}, \end{cases} \tag{4}$$

where, $\phi_{c,k}$ is now the threshold volume fraction for the onset of thermal percolation, and p and q are critical exponents in

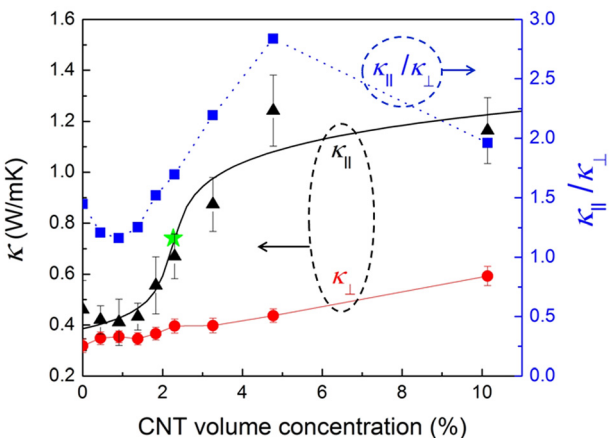

FIG. 3. The variation of the measured thermal conductivity with added CNT filler concentration depicted for the *in plane* ($\kappa_{\parallel}$) and *cross plane* ($\kappa_{\perp}$) configurations. The anisotropy ratio, i.e., $\kappa_{\parallel}/\kappa_{\perp}$ is indicated on the right hand axis. The * indicates the results of the Straley model relating the product of the *thermal* resistances of the matrix and the filler to the percolation threshold.

the respective regimes. We obtained, experimentally, a $\phi_{c,k} \sim 2.2$ vol. %, close to the theoretically expected value, with $p \sim 0.2$ and $q \sim 0.1$. The value of the exponents in the power laws depends on the particular type of conductivity[14,20] (i.e., electrical or thermal) as well as on the ratio of the respective conductivities of the constituent phases.[21]

The concomitant larger variation in the increase of the σ (ten-twelve orders of magnitude for $\sigma_\perp$ and $\sigma_\parallel$) of the CNT/polymer composites compared to the increase of the κ (50% and 400% for $\kappa_\perp$ and $\kappa_\parallel$, respectively) may be attributed to the intrinsically greater range in electrical conductivity. In the former case, one has to consider the much lower electrical resistance of the CNTs compared to the polymers, while there is generally a much smaller variation in κ between disparate materials. The substantial enhancement in $\kappa_\parallel$ compared to $\kappa_\perp$ is also to be noted. We ascribe the $\kappa_\parallel$ increase to the effects of percolation. Further evidence was obtained through adapting a Straley model[22] (used for determining the critical exponents for the conductivity of random resistor lattices), where the filler (R_f) and matrix (R_m) could be represented as *thermal* resistors. Through such modeling, the effective thermal conductivity at the percolation threshold fraction could be related to $R_f^u R_m^{1-u}$, where $u = \frac{p}{p+q}$, and the estimated value has been indicated through a * in Figure 3. The equivalent σ values, where the filler and the matrix were represented as *electrical* resistors, have been indicated through the * symbol in Figure 2.

We model such connectivity effects encompassing *both* electrical and thermal conductivity, through a two-dimensional model considering the total number of percolating networks in the *in plane* and *cross plane* directions, contributing to an equivalent resistance, $R_\parallel$ and $R_\perp$, respectively. Following the schematic in Figure 4, we assume that each network is comprised of a series of nanotubes, and many such networks yield a nanostructure contributed total resistance in the *in-plane* direction ($R_{CNT,\parallel}$). Conduction would occur simultaneously through the polymer matrix of resistance $= R_{M,\parallel}$. If the resistance of a single nanotube, $R_c = \frac{l}{A_c \sigma_c}$, with l being the average nanotube length, A_c the cross-sectional area, and σ_c the conductivity (which should now be interpreted as an electrical: σ *or* thermal conductivity: κ) with an interfacial resistance, R_i (in units of $\Omega\,\mathrm{m}^2$), then $R_{CNT,\parallel}$ would be

$$\frac{1}{R_{CNT,\parallel}} = \frac{1}{\left(R_c + \frac{R_i \cos(\theta)}{A_c}\right)} \frac{L_\parallel}{l\cos(\theta)} \frac{N_C l \cos(\theta)}{L_\parallel}. \quad (5)$$

θ is an average orientation angle between the CNT longitudinal axis and the horizontal, $L_\parallel$ is the length of the composite sample, and N_c indicates the total number of CNTs as estimated through the incorporated volume fraction (ϕ). The second multiplicative term on the right is a measure of the number of horizontal networks. The $R_{M,\parallel} = \frac{L_\parallel}{A_\parallel (1-\phi)\sigma_m}$, where $A_\parallel$ is the composite cross-sectional area and σ_m is the matrix (/polymer) conductivity. The *net in-plane* conductivity ($\sigma_\parallel$) constituted of $R_{CNT,\parallel}$ and $R_{M,\parallel}$ would be

$$\sigma_\parallel = \frac{\phi \cos^2(\theta)}{\left(\frac{1}{\sigma_c} + \frac{R_i \cos(\theta)}{l}\right)} + (1-\phi)\sigma_m. \quad (6)$$

Through similar methodology, the *net cross-plane* conductivity ($\sigma_\perp$) constituted of $R_{CNT,\perp}$ and $R_{M,\perp}$ would be

$$\sigma_\perp = \frac{\phi \sin^2(\theta)}{\left(\frac{1}{\sigma_c} + \frac{R_i \sin(\theta)}{l}\right)} + (1-\phi)\sigma_m. \quad (7)$$

Assuming a range of θ (i.e., $|\theta| < \theta_b$) and a constraint on the anisotropy ratio between the *in-plane* and the *cross-plane* conductivity, i.e., $\frac{\langle\sigma_\parallel\rangle}{\langle\sigma_\perp\rangle} \to 1$,as $\theta_b \to \pi/2$, we derive:

$$\frac{\langle\sigma_\parallel\rangle}{\langle\sigma_\perp\rangle} = \frac{\theta_b + \sin(\theta_b)\cos(\theta_b) + \left(\frac{1-\phi}{\phi}\right)\left(\frac{1}{\sigma_c} + \frac{2R_i \sin(\theta_b)}{l}\right)\sigma_m}{\theta_b - \sin(\theta_b)\cos(\theta_b) + \left(\frac{1-\phi}{\phi}\right)\left(\frac{1}{\sigma_c} + \frac{2R_i \sin(\theta_b)}{l}\right)\sigma_m}. \quad (8)$$

In the case of electrical conductivity, due to the measured small σ_m ($\sim 3 \times 10^{-12}\ \Omega^{-1}\mathrm{m}^{-1}$), we could ignore the expressions on the far right hand side of the numerator and denominator, whence we obtain

$$\frac{\langle\sigma_\parallel\rangle}{\langle\sigma_\perp\rangle} \cong \frac{\theta_b + \sin(\theta_b) + \cos(\theta_b)}{\theta_b - \sin(\theta_b) + \cos(\theta_b)}. \quad (9)$$

Inserting the corresponding $\sigma_\perp$ and $\sigma_\parallel$ from Figure 2, at $\phi > \phi_c$ (i.e., at 3.3 vol.%, 4.8 vol.%, and 10 vol.%), we find the θ_b values to be 4.6°, 8.5°, and 19°, respectively. These values were then used for interpreting the thermal conductivity variation *vis-à-vis* the percolation like behavior of $\kappa_\parallel$.

However, for modeling the thermal conductivity anisotropy, $\frac{\langle\kappa_\parallel\rangle}{\langle\kappa_\perp\rangle}$ the matrix conductivity, κ_m ($\sim 0.3\,\mathrm{W/mK}$) cannot be neglected, and terms involving the thermal interfacial resistance (R_i^{th} in units of $\mathrm{m^2K/W}$) would remain

$$\frac{\langle\kappa_\parallel\rangle}{\langle\kappa_\perp\rangle} = \frac{\theta_b + \sin(\theta_b)\cos(\theta_b) + \left(\frac{1-\phi}{\phi}\right)\left(\frac{1}{\kappa_c} + \frac{2R_i^{th} \sin(\theta_b)}{l}\right)\kappa_m}{\theta_b - \sin(\theta_b)\cos(\theta_b) + \left(\frac{1-\phi}{\phi}\right)\left(\frac{1}{\kappa_c} + \frac{2R_i^{th} \sin(\theta_b)}{l}\right)\kappa_m}. \quad (10)$$

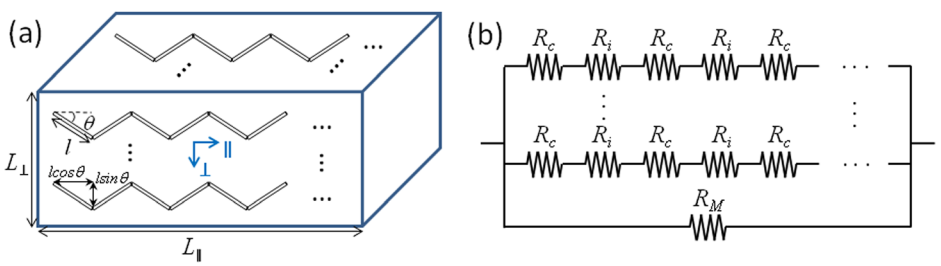

FIG. 4. (a) Modeling networks of aligned MWCNTs in the polymer matrix, and (b) the equivalent electrical/thermal circuit schematic with R_c as the nanotube resistance and R_i as the interfacial resistance.

Along with the corresponding $\kappa_{\|}$ and $\kappa_{\perp}$ from Figure 3, the θ_b values obtained previously were inserted into Eq. (10), to consistently estimate a κ_c ($\sim$240 W/mK) and an R_i^{th}($\sim 7 \times 10^{-8}$ m^{2}K/W). Such estimates are in excellent accord with previous evaluations of nanotube interfacial thermal resistance[23] and further indicate a significant modulation of the thermal conductivity of nanostructures, when they are dispersed into a matrix. While previous reports[24,25] indicated a lack of percolation[26] due to (i) the relatively low thermal conductivity contrast and (ii) the interfacial resistance between the conducting nanostructure and the matrix (polymer), we have then seen that percolation behavior is indeed possible. In such previous studies, e.g., it was concluded based on theoretical analysis (based on the finite element method: FEM and molecular dynamics) that the low thermal conductivity contrast (of less than 10^4) between the matrix and the filler precludes percolation. A linear variation of the thermal conductivity with volume fraction was predicted based on effective medium theory, which may not be valid at/near the percolation threshold.[10,27] Single walled nanotube-epoxy composites were studied,[25] where the random orientation of the nanotubes was thought to be the reason for the thermal conductivity increase. Indeed, a greater degree of isotropy would imply a lower percolation threshold as was indicated in Figure 2. Additionally, previous work[25,26] did not consider the effects of interfacial resistance between the nanotubes and the matrix, the effects of which have been discussed in much more detail in this paper.

We have then shown that it is feasible to adapt a synthesis methodology, e.g., using stacking of nanotube/polymer composite sheets, facilitating percolation behavior. We surmise that an increased nanotube aspect ratio, enhanced from that presented in this paper, would yield a corresponding exponential increase of the thermal conductivity.

In summary, we have shown, through detailed experiments and modeling, evidence of anisotropy in both the electrical and thermal conductivity in nanotube/polymer composites. A power law relation for the thermal conductivity has been indicated, indicative of percolation-like behavior, with implications for tunable thermal conductivity and thermal switching.

The support from the National Science Foundation (Grant Nos. ECS 0643761 and CMMI 1246800) is acknowledged. Interactions and discussions with S. Pfeifer (General Atomics) are deeply appreciated.

[1]S. Berber, Y.-K. Kwon, and D. Tomanek, Phys. Rev. Lett. **84**, 4613–4616 (2000).
[2]P. R. Bandaru, J. Nanosci. Nanotechnol. **7**, 1239–1267 (2007).
[3]L. Ci, J. Suhr, V. Pushparaj, X. Zhang, and P. M. Ajayan, Nano Lett. **8**, 2762–2766 (2008).
[4]D. D. L. Chung, Carbon **39**, 279–285 (2001).
[5]D. M. Bigg and D. E. Stutz, Polym. Compos. **4**, 40–46 (1983).
[6]M. Hughes, *Dekker Encyclopedia of Nanoscience and Nanotechnology* (Taylor & Francis, London, 2004), pp. 447–459.
[7]S. Pfeifer and P. R. Bandaru, "A method for quantitatively characterizing the dispersion of nanostructures in polymer composites," Polymer (in press).
[8]S.-H. Park, P. Theilmann, P. Asbeck, and P. R. Bandaru, IEEE Trans. Nanotechnol. **9**, 464–469 (2010).
[9]S.-H. Park, P. Thielemann, P. Asbeck, and P. R. Bandaru, Appl. Phys. Lett. **94**, 243111 (2009).
[10]S. Kirkpatrick, Rev. Mod. Phys. **45**, 574–588 (1973).
[11]S. Pfeifer, S. H. Park, and P. R. Bandaru, J. Appl. Phys. **108**, 024305 (2010).
[12]I. Balberg, C. H. Anderson, S. Alexander, and N. Wagner, Phys. Rev. B **30**, 3933–3943 (1984).
[13]A. Celzard, E. McRae, C. Deleuze, M. Dufort, G. Furdin, and J. F. Mareche, Phys. Rev. B **53**, 6209–6214 (1996).
[14]D. Stauffer and A. Aharony, *Introduction to Percolation Theory* (CRC Press, Boca Raton, FL, 1994).
[15]S. L. White, B. A. DiDonna, M. Mu, T. C. Lubensky, and K. L. Winey, Phys. Rev. B **79**, 024301 (2009).
[16]F. Du, J. E. Fischer, and K. L. Winey, Phys. Rev. B **72**, 121404(R) (2005).
[17]D. G. Cahill, Rev. Sci. Instrum. **61**, 802–808 (1990).
[18]H. S. Carslaw and J. C. Jaeger, *Conduction of Heat in Solids*, 2 ed. (Oxford University Press, New York, 1986).
[19]T. Borca-Tasciuc, A. R. Kumar, and G. Chen, Rev. Sci. Instrum. **72**, 2139–2147 (2001).
[20]M. Foygel, R. D. Morris, D. Anez, S. French, and V. L. Sobolev, Phys. Rev. B **71**, 104201 (2005).
[21]B. I. Shklovskii and A. L. Efros, *Electronic Properties of Doped Semiconductors* (Springer-Verlag, New York, NY, 1984).
[22]J. P. Straley, Phys. Rev. B **15**, 5733–5737 (1977).
[23]S. T. Huxtable, D. G. Cahill, S. Shenogin, L. Xue, R. Ozisik, P. Barone, M. Usrey, M. S. Strano, G. Siddons, M. Shim, and P. Keblinski, Nature Mater. **2**, 731–734 (2003).
[24]N. Shenogina, S. Shenogin, L. Xue, and P. Keblinski, Appl. Phys. Lett. **87**, 133106 (2005).
[25]M. J. Biercuk, M. C. Llaguno, M. Radosavljevic, J. K. Hyun, A. T. Johnson, and J. E. Fischer, Appl. Phys. Lett. **80**, 2767–2769 (2002).
[26]P. Bonnet, D. Sireude, B. Garnier, and O. Chauvet, Appl. Phys. Lett. **91**, 201910 (2007).
[27]R. Landauer, AIP Conf. Proc. **40**, 2–45 (1978).